AIMS Materials Science, 7(3): 269–287.
DOI: 10.3934/matersci.2020.3.269
Received: 12 February 2020
Accepted: 21 May 2020
Published: 01 June 2020

http://www.aimspress.com/journal/Materials

Research article

Sustainable green chemical synthesis of discrete, well-dispersed silver nanoparticles with bacteriostatic properties from carrot extracts aided by polyvinylpyrrolidone

Purabi R. Ghosh[1], Derek Fawcett[1], Michael Platten[2], Shashi B. Sharma[2], John Fosu-Nyarko[3] and Gerrard E. J. Poinern[1,*]

[1] Murdoch Applied Nanotechnology Research Group, Department of Physics, Energy Studies and Nanotechnology, School of Engineering and Energy, Murdoch University, Murdoch, Western Australia 6150, Australia
[2] Department of Primary Industry and Regional Development, 3 Baron Hay Court, South Perth, Western Australia 6151, Australia
[3] Plant Biotechnology Research Group, Western Australian State Agricultural Biotechnology Centre, College of Science, Health, Engineering and Education, Murdoch University, Murdoch, Western Australia 6150, Australia

* **Correspondence:** Email: G.Poinern@murdoch.edu.au; Tel: +61893602892.

Abstract: Large amounts of food products are disposed of around the world because they are below market standards. In Australia, low value, non-marketable carrots (*Daucus carota*) are ploughed into farmlands as green manure or are treated as waste. In recent years significant research interest has focused on developing waste valorisation strategies using new green chemistry-based sustainable processes. More importantly, strategies that also provide solutions for emerging challenges like the rising reports of resistance of bacteria to existing microbes are favourable. This study explored a facile synthesis process to reduce aqueous silver ions in aqueous carrot extracts to form silver nanoparticles that may have antibacterial properties. The synthesis process produced particles with surface plasmon resonance peaks typical of crystalline silver. The silver nanoparticles produced from pure carrot extracts were spherical and pseudo-spherical, 2 to 25 nm wide. However, with polyvinylpyrrolidone, much wider (10–50 nm), well-dispersed silver nanoparticles of various shapes including spherical, polygonal, rod-like and triangular types were produced. Several biomolecules which may act as

reducing and capping agents for the process were identified; they included ascorbic, gallic and chlorogenic acids. The Ag nanoparticles produced significant zones of inhibition against the gram-negative *E. coli* and gram-positive *S. epidermidis*, indicating they had bacteriostatic properties. The study demonstrates that producing Ag nanoparticles with antibiotic properties from carrots is a good valorisation strategy because other uses for rejected carrot produce such as application as green manure may not be interrupted.

Keywords: green chemistry; silver nanoparticles; sustainability; antibacterial; carrot extracts

1. Introduction

Nanoparticles currently have broad applications in many industries; this is evident from the considerable research interest it has generated in recent years [1–3]. These applications are in biomedical, animal and plant researches where their ability to increase transfection of DNA of animal and plant cells are explored [4,5]. In the pharmaceutical industry and medicine, the use of nanoparticles as drug delivery systems for small and large molecules has been explored. For some applications, especially in the various fields of drug applications, essential features of desirable nanoparticle systems include particle size and distribution, dispersion, surface properties and loading capacity. These properties determine their effective distribution, fate, toxicity and penetrability in biological targets. In terms of drug delivery, nanoparticle systems are preferred to microparticles because of the former's superiority in influencing intracellular uptake, drug loading and release, and stability in biological systems. Nanoparticles can be synthesised from several sources including polysaccharides proteins, and synthetic polymers and the choice of synthesis methods usually depend on the particle size, shape and composition desired. The methods include polymerisation of monomers; ionic gelation or coacervation of hydrophilic polymers, dispersion of preformed polymers, particle replication in non-wetting templates and supercritical fluid technology. The potential of nanoparticles in fighting the rising development of antibiotic resistance has had limited research.

Bacteria resistance to current antibiotics is on the increase, and this development is one of the most serious health threats to humanity today [6–8]. Lack of effective antibiotics can lead to delayed recovery from infections, therapy failure and even loss of lives. Meanwhile, the discovery of new antibiotics has steadily declined in recent years. Resistance is caused by genetic mutation or is acquired from other bacteria. Alternative sources of materials are needed to develop new antibiotics using non-toxic and eco-friendly manufacturing processes [9,10]. Such materials should have physicochemical properties that are broad and effective enough to interfere with the structure and cellular functions of many strains of pathogenic bacteria [11]. One such source is metal nanoparticles which have unique mechanical, chemical, magnetic, optical or electrical properties that make them better adapted to many applications than bulk materials [12,13]. In particular, silver (Ag) nanoparticles have attracted significant interest due to its antimicrobial, antioxidant and anti-inflammatory properties, which has resulted in its incorporation into several pharmaceutical preparations [14,15]. Manufacture of metal nanoparticles has traditionally used physical and chemical processes and materials that are harmful to both humans and the environment [16]. Some of these processing

materials consist of surfactants employed as sculpturing agents, or as capping agents that stabilise nanoparticles and prevent them from clustering. Nanoparticle toxicity can also arise from surface contaminants deposited during synthesis [17]. The level of toxicity can be exacerbated by the high surface energy of nanoparticles which can cause its surface to be coated by atoms in the surrounding environment [18,19]. One of the factors that may increase the uptake of such nanoparticles is the cost and ease of synthesis.

In recent years, organic products such as fruits and vegetables have been used as sources of renewable chemical compounds for high-value chemical and pharmaceutical products [20]. Such food resources contain a diverse range of biomolecules such as alkaloids, phenolics, proteins, polysaccharides and terpenoids; these can promote nucleation leading to the formation of stable metal nanoparticles [21]. In Australia, 30–40% of food products are discarded because they do not meet quality standards set by the retail sector and consumers. In the case of carrots, the rejects with no commercial value are either too large to bag and sell or are bruised [22]. For example, in the Australian state of Tasmania alone, a reported 150 tonnes of healthy carrots are ploughed back into farmlands each year [22]. The high amounts of carrot which are under-utilised make it an ideal candidate for a valorisation strategy which involves its use for green synthesis of Ag nanoparticles. This potentially economically viable venture will potentially add to the AUS$9.0 billion dollars the sale of fruits and vegetables already contributes to the Australian economy [23]. Using carrot extracts not only avoids coating the nanoparticles with harmful chemicals and solvents but could also generate a synergistic effect produced by the chemical constituents present in the extracts.

Ag nanoparticles have been synthesised successfully from several plant sources [24–27]. Ag nanoparticles synthesised from carrot extracts are reportedly mostly spherical, between 4 and 20 mm in diameter and are usually highly agglomerated [26,27]. There is currently very little information available on the biomolecules that may be acting as reducing agents in the synthesis of Ag nanoparticles. Besides, the antimicrobial properties of these Ag nanoparticles are not known. In this study, we employed a facile and green chemistry-based method to synthesise discrete, well-dispersed Ag nanoparticles from carrot extracts at room temperature. The innovation of this study is in the use of polyvinylpyrrolidone (PVP) as a modelling agent to promote the growth of the synthesised Ag nanoparticles along specific crystal faces. The unique features of the Ag nanoparticles produced were characterised using UV-visible spectroscopy, X-ray diffraction spectroscopy, high-performance liquid chromatography, Fourier-transform infrared spectroscopy and transmission electron microscopy. Also, the antimicrobial properties of the Ag nanoparticles were investigated using the gram-negative *Escherichia coli* and gram-positive *S. epidermidis*, both of which are usually part of the normal human biota [28]. In recent years, *S. epidermidis* has been shown to compromise the immune system of patients receiving intravenous catheters and medical prostheses in some hospitals, and *E. coli* has been associated with food poisonings [29,30]. The outcome of this research lays a foundation for deriving value in the form of Ag nanoparticles from carrots which would otherwise be wasted or used as green manure in Australia. This valorisation strategy could also be applied to many food products in the same category as carrots to produce useful nanoparticles with broad applicability in the pharmaceutical and other industries.

2. Materials and methods

2.1. Materials

Fresh and healthy carrots used in the study were purchased from a local supermarket in Perth, Western Australia. All chemicals used in this work were supplied by Sigma-Aldrich (Castle Hill, NSW Australia) and used without further modifications. Milli-Q® water produced from Ultrapure Water System (D11931 Barnstead, 18.3 $M\Omega \cdot cm^{-1}$) supplied by Thermo Scientific, Australia was used in all experiments.

2.2. Preparation of carrot extract

The leafy green tops of the carrots were removed, and the outer layer scraped with a knife. The peeled carrot was scrubbed and washed several times with Milli-Q® water to remove surface contaminants. After cleaning, 100 g of the carrots were chopped into small pieces (1 cm^3) and crushed in a standard domestic mixer with 200 mL of Milli-Q® water (mass ratio 1:2). The suspension was then poured into the blending bowl of an IKA T25 Digital Ultra-Turrax® Homogenizer (IKA, Germany) and was further homogenized at 5000 rpm for 5 min at room temperature (24 °C). The suspension was then filtered three times: the first was done with a Hirsch funnel fitted with a filter to remove the bulk of the carrot pulp leaving a smooth orange solution. The filtrate was then passed through a 0.22 μm Millex® (33 mm diameter.) syringe filter unit twice. Changes in the colour of the carrot extract during filtration are presented in Figure 1a. After filtration, the extract stock solution was kept into a glass beaker at room temperature until it was used in designated experiments.

2.3. Green synthesis of silver nanoparticles from carrot extract

The green synthesis of Ag nanoparticles simply involved the addition of a 1 mL aqueous solution of 0.1 M $AgNO_3$ (99.99% purity) to a glass vial containing a 1 mL of the carrot extract (volume ratio of 1:1) followed by a thorough mixing for 1 min. The solution was then allowed to stand at room temperature (24 °C) for 20 min. During that time, the homogenous solution changed colour from yellow to pale brown, indicating the formation of Ag nanoparticles, as shown in Figure 1b.

2.4. Synthesis of silver nanoparticles with carrot extract and modelling agent

The modelling agent used in this study was the water-soluble Polyvinylpyrolidine (PVP) (molecular weight 44000 $g \cdot mol^{-1}$). The effect of four concentrations of PVP on the physicochemical properties of the synthesised Ag nanoparticles was assessed; 0.5, 1.0, 1.5 and 2.0%. To each PVP concentration, carrot extract and silver nitrate solutions were added in a volume ratio of 1:1:1. The solutions were then mixed for 1 min and then allowed to stand at room temperature for 20 min. Completion of the synthesis of Ag nanoparticles was typified by the change in colour of the solution from yellow to brown (Figure 1b).

2.5. Nanoparticle characterisation studies

The particle sizes, shapes, compositions of the nanoparticles formed and the presence of functional groups in the bio-reaction mixtures were investigated using several techniques and instruments including UV-visible and X-ray diffraction spectroscopy, Fourier-Transform Infrared Spectroscopy (FTIR), High-Performance Liquid Chromatography (HPLC) and Transmission Electron Microscopy (TEM).

2.5.1. UV-visible spectroscopy

Bio-reduction of Ag^+ ions produced from the different synthesis methods was assessed at room temperature via UV-visible spectroscopy (Varian Cary 50 series UV-Visible spectrophotometer, Australia) over a spectral range between 200 and 800 nm, with a spectral resolution at 1 nm.

2.5.2. X-ray diffraction spectroscopy

The crystalline structure of the synthesized nano-crystalline powders was characterised using X-ray diffraction spectroscopy using a Bruker D8 series diffractometer [Cu Kα = 1.5406 Å radiation source] (Bruker, USA) operating at 35 kV and 28 mA. Diffraction patterns were collected over a 2θ range starting at 20° and finishing at 90°. The scanning procedure incorporated flat plane geomet, with an incremental step size of 0.02° and an acquisition time of 2 s. The liquid samples were extracted from individual glass vials using a clean glass pipette fitted with a rubber bulb. Two to three drops were taken from each glass vial, then deposited and dispersed on individual glass microscope slides. The slides were dried under vacuum for 4 h at room temperature. The observed Bragg peak positions recorded in the respective diffraction patterns were compared with those reported in the ICDD (International Centre for Diffraction Data) databases and the appropriate Miller indices were assigned to the respective peaks.

2.5.3. Fourier-Transform Infrared Spectroscopy (FTIR)

FTIR was used to identify the major functional groups and vibration modes present in the pure carrot extracts and the various reaction mixtures. FTIR was carried out using a Perkin–Elmer Frontier FTIR spectrometer (Perkin–Elmer, Germany) fitted with a universal Single bounce Diamond ATR attachment that was used to analyze samples over a wavelength range starting at 525 cm^{-1} up to a maximum of 4000 cm^{-1} in steps of 4 cm^{-1}.

2.5.4. High-Performance Liquid Chromatography (HPLC)

Further analysis of phenolic compounds was undertaken using the HPLC technique: this was done using a Shimadzu Prominence Modular HPLC (Shimadzu, Japan). The unit was equipped with an Apollo C18 5u column (150 × 4.60 mm supplied by Grace), an LC-20AT degasser, a SIL-20A/C HT auto-sampler and a CTO-20A/C column oven with an operating range from 4 to 85 °C, an

SPD-20AV UV detector with a wavelength range from 190 to 900 nm and an SPD-M20A diode-array detector with an operational range from 190 to 800 nm. Mobile phases used were acidic waters (A) 0.1% ortho-phosphoric acid and (B) 0.1% acetonitrile-ortho-phosphoric acid. The operational flow rate was 0.8 mL/min, and optimal separation temperature was achieved at 35 °C using the elution gradient of 95% B at 0 min and then ranging from 95% down to 50% over a retention period ranging between 0 and 30 min. Retention times and spectral characteristics of each compound were compared to commercial standards for Chlorogenic acid isomers 3,5-dicaffeoylquinic acid and 5-O-caffeoylquinic acid (neochlorogenic acid).

2.5.5. Transmission electron microscope (TEM)

TEM images showing particle size and morphology were taken using a Technai G2, FEI, Electron Optics (G2, FEI, USA). The TEM was fitted with a W-source and an ultra-high-resolution pole piece operating at 200 kV. TEM sample preparation consisted of a single droplet taken from a diluted solution derived from extracts containing Ag nanoparticles. The droplet was placed on a carbon-coated copper grid and, allowed to dry (by evaporation) at room temperature. The dried sample was placed onto the specimen holder and loaded into the TEM for analysis.

2.6. Testing the antibacterial activity of biosynthesized Ag nanoparticles

The antibacterial activity of the biosynthesized Ag nanoparticles was investigated using the Kirby and Bauer sensitivity method [28]. The method was used against two bacterial pathogens, the gram-negative *Escherichia coli* (Migula 1895; Castellani & Chalmers 1919) and the gram-positive *Staphylococcus epidermidis* (Winslow & Winslow 1908; Evans 1916). The bacteria were cultured in Petri dishes (90 mm diameter) containing a nutrient agar medium consisting of 5 g of peptone, 3 g of beef extract, 15 g of agar, and 5 g of sodium chloride per litre made with of distilled water and adjusted to pH 6.8 at 25 °C. Culturing involved uniformly spreading 100 μL of liquid cultures on the solid media using a sterile cotton swab. The cultures were then incubated at 37 °C in an oven for 2 h to settle. Three treatments each were set up for the two bacterial cultures. After heating, 6 mm diameter sterile disks (Whatman® AA 2017-006, (Merck, Germany) were placed on the agar media with bacterial cultures using sterile forceps. Then using a micropipette, 20 μL of each of the three treatments were deposited onto an individual sterile disk and then allowed to air dry for 20 min. The treatments were: (1) carrot extract, (2) $AgNO_3$ + carrot extract and (3) $AgNO_3$ + carrot extract + PVP mixture. Once the mixture dried, the dishes were incubated in an oven for 24 h at 37 ºC. Each treatment was carried out in triplicates for each bacterial type. The diameters of the zones of inhibition were then measured, and the means and standard errors calculated.

3. Results and discussions

3.1. Detection of Ag nanoparticles using UV-visible absorption spectroscopy

UV-visible absorption spectroscopy is an established technique for detecting Ag nanoparticles

present in colloids. The technique is sensitive and can detect intense absorption peaks due to the collective excitation of conduction electrons in spherical metal nanoparticle samples (surface plasmon resonance-SPR). The absorption peak or SPR depends on the particle size and the dielectric medium of the surrounding extract. The colour of the initial carrot extract after filtration was a pale yellow. The extract and $AgNO_3$ mixture (volume ratio 1:1) changed from pale yellow to orange-brown 20 min after mixing. The resulting colour change was credited to the excitation of the SPR during the formation of Ag nanoparticles in the mixture (Figure 1b). The UV-visible absorption spectrum of the carrot extract and $AgNO_3$ mixture showed a spread in the range 350 to 565 nm with a peak typically around 412 nm. This observation corresponded to Mie's theory, which predicts a single SPR band in the absorption spectra for spherical metal nanoparticles. If there were two or more SPR peaks, this would have indicated anisotropic particles [31]. The observed broad peaks suggest there was a variation in the size distribution of the particles [32–34].

The effect of 1.0% and 2% PVP as a modelling agent during the synthesis of the Ag nanoparticles was also investigated. For these reactions, the colour changes also occurred within 20 min and were consistent with the transition from pale-yellow to brown as in Figure 1b. However, there was a wider spread of the UV-visible absorption spectra, between 350 nm to about 615 nm with a pronounced peak at 415 nm. The position of the maximum absorption wavelength did not change much from the samples without PVP, and the pronounced SPR also indicated the Ag nanoparticles had a narrow size distribution (Figure 1c).

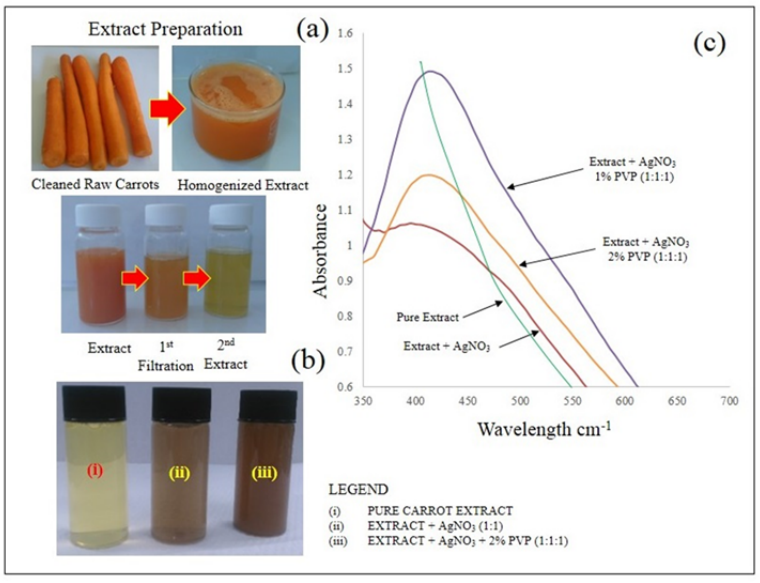

Figure 1. Biosynthesis of Ag nanoparticles (a) Variation in colour of carrot extract during filtration, (b) variation between the volume ratio-based reaction mixtures, and (c) a selection of UV-visible absorption spectroscopy data for various reaction mixtures.

3.2. Crystallography of the synthesised Ag nanoparticles

The crystalline nature of the biologically synthesised Ag nanoparticles was investigated using XRD spectroscopy. A representative XRD diffraction pattern of the dried carrot extract obtained from the filtrate is presented in Figure 2. The XRD pattern reveals (2θ range of 20° to 90°) a predominantly amorphous material, apart from an unassigned peak that was observed around 77°. The presence of this peak suggests there was some degree of crystallization of a bio-organic phase. A typical diffraction pattern for Ag nanoparticles synthesized using carrot extract was present, as shown in Figure 2b and showed four distinct Bragg reflection peaks at 37.77°, 44.00°, 63.99° and 77.83°. The four peaks were indexed as (111), (200), (220) and (311) reflection planes respectively and corresponded to the face-centred cubic (fcc) structure of Ag phases. These face-centred cubic structures matched those reported in the database of the Joint Committee on Powder Diffraction Standards (JCPDS No 04-0783) for pure crystalline Ag particles. The diffraction peaks were also subject to broadening, which was credited to the particle size effect resulting from the small particle sizes produced by the bio-reduction process [35]. The broadening is also indicative of experimental conditions which encouraged crystal nucleation and growth. The crystalline size, $t_{(hkl)}$, of Ag nanoparticles was calculated from the following Debye–Scherrer Eq 1 below:

$$t_{(hkl)} = \frac{0.9\lambda}{B\cos\theta_{(hkl)}} \tag{1}$$

where λ is the wavelength of the monochromatic X-ray beam, B is the Full Width at Half Maximum (FWHM) of the peak at the maximum intensity, $\theta_{(hkl)}$ is the peak diffraction angle that satisfies Bragg's law for the *(h k l)* plane and $t_{(hkl)}$ is the crystallite size. Analysis of the diffraction pattern revealed that the bio-reduced Ag nanoparticles had a well-defined crystalline structure. The mean crystallite size was estimated using the FWHM of the (111) peak and was calculated to be 25 nm. Also, two less-pronounced peaks were seen in the diffraction pattern at 27.9° and 81.9° (Red Triangles in Figure 2). The presence of these two peaks suggests there was also some crystallization of some bio-organic phases present on the surface of the Ag nanoparticles. The peak located at 27.9° was due to ascorbic acid present in the carrot extract and matched the standard data file at the JCPDS database, No 22-1536, while the peak located at 81.9° could not be defined.

The effect of PVP in the bio-reduction process is shown in the diffraction patterns for reaction mixtures containing 0.5, 1.0, 1.5 and 2.0% PVP presented in Figure 2 as c, d, e, and f respectively. The peaks in the respective diffraction patterns were consistent with those of crystalline Ag particles. The mean crystallite size for the four diffraction patterns was calculated using the width of the (111) peak and were found to be 15 nm (0.5% PVP), 11 nm (1.0% PVP), 13 nm (1.5% PVP) and 16 nm (2.0% PVP). These crystallite sizes were consistently smaller than the mean 25 nm calculated for those synthesised without PVP. Also, the intensity of the peaks tended to decline with increasing PVP content in the reaction mixtures indicating PVP acted as a surface stabilizer and growth modifier.

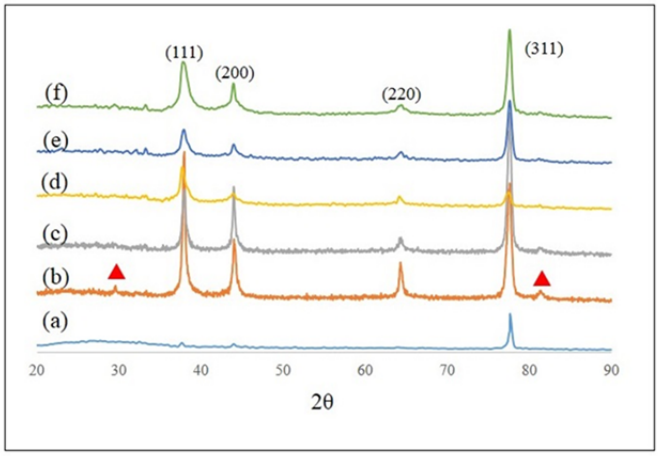

Figure 2. Crystallography of carrot extract and synthesised Ag nanoparticles: (a) Carrot extract; (b) Ag nanoparticles produced from the bio-reduction of $AgNO_3$ and carrot extract; (c–e) Ag nanoparticles produced from bio-reduction of $AgNO_3$ and carrot extract incorporating different concentrations of PVP (c) 0.5%, (d) 1.0%, (e) 1.5% and 2.0%.

3.3. Identification of possible reducing agents involved in the biosynthesis of Ag nanoparticles

The carrot extract was suspected to contain a variety of components that can act as bio-reducing agents. Such agents may reduce the energy barrier for the reduction of Ag^+ ions to Ag^0 metal atoms whereas other components can act as capping agents to stabilize and prevent the aggregation of the synthesized Ag nanoparticles. Analysis of XRD data revealed the presence of ascorbic acid on the bio-reduced Ag nanoparticles. HPLC was therefore used to investigate the possible involvement of ascorbic acid and components such as gallic acid and chlorogenic acids present in the carrot extract. HPLC is widely used to determine a wide variety of chemical components present in fruits, vegetables and plant biomass [25,36]. For example, HPLC can detect phenolic acids, sugars and different levels of chemical components specific to particular carrot cultivars [37,38]. This study investigated ascorbic, gallic and chlorogenic acids as potential reducing and capping agents. Chlorogenic acid is an ester produced from caffeic acid and the 3-hydroxyl position of L-quinic acid. There are several isomers of chlorogenic acid. Two isomers, namely, 3,5-dicaffeoylquinic acid and 5-O-caffeoylquinic acid (neochlorogenic acid, were investigated in this study. A representative chromatogram is presented in Figure 3, which shows the chlorogenic isomers identified by their respective retention times. The retention time recorded for 5-O-caffeoylquinic acid was 13.4 min, while that for 3,5-dicaffeoylquinic acid was 23.9 min. Both retention times compared well with the respective reference standards. Also indicated in Figure 3 are the peaks and retention times for ascorbic acid and gallic acid.

Despite chlorogenic acid isomers being present in the carrot extract (Figure 3), it is unlikely they are the main drivers for the bio-reduction of $AgNO_3$. Studies using chlorogenic acid as the reducing agent for the synthesis of Ag nanoparticles from $AgNO_3$ have shown temperatures around 80 °C are needed and incubation times can be as long as ten hours [39,40]. The present work has shown bio-reduction was rapid (less than 20 min) and occurred at room temperature (24 °C) reducing

the likelihood of the acid's involvement in the bio-reduction process. It has been shown that oxidation of phenol groups in gallic acid is responsible for bio-reduction of $AgNO_3$ in the generation of spherical nanoparticles ranging from 7 to 89 nm [37]. The bio-reduction process took more than 30 min at 80 °C, and a quinoid compound with a keto-enol-system was absorbed onto the surface of the Ag nanoparticles. This capping agent stabilised the synthesised nanoparticles [38,39]. Like the chlorogenic acid, the contribution of the gallic acid to the bio-reduction process at room temperature was believed to be limited. In studies where Ag nanoparticles have been synthesised from carrot extracts at room temperature, ascorbic acid was identified as the primary reducing agent [27]. The authors also reported that pure ascorbic acid could reduce $AgNO_3$ at room temperature over a similar time frame as pure carrot extracts, which also confirms the results reported by [27]. Since the reactions involving both the gallic and chlorogenic acids need to be around 80 °C to initiate the reduction process, it can be inferred that the ascorbic acid present in the carrot extract is the predominant reducing agent at room temperature whereas the most probable capping agent is the ascorbate radicals produced during the reduction process [41]. However, oxidation reactions produced by phenol groups in gallic acid can also be responsible for the reduction and subsequent stabilisation of Ag^+ ions [42].

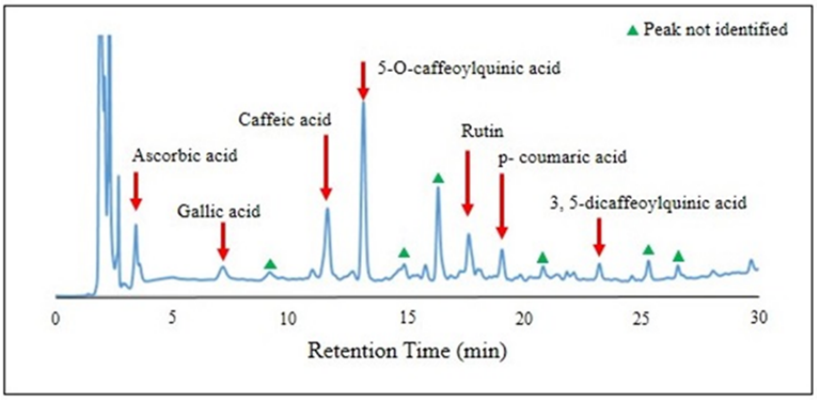

Figure 3. High-performance liquid chromatographic showing peaks and retention times characteristic of the presence of two chlorogenic acid isomers, 3,5-dicaffeoylquinic acid and 5-O-caffeoylquinic acid, and those for ascorbic acid, gallic acid, caffeic acid, rutin and p-coumaric acid.

3.4. Influence of PVP in stabilising Ag nanoparticles synthesised from carrot extracts

FTIR Spectroscopy was used to further characterise biomolecules present in the carrot extract by assessing their roles in reducing the $AgNO_3$ to form stabilised Ag nanoparticles. The FTIR spectra were recorded before and after adding $AgNO_3$ and PVP to respective carrot extract-based reaction mixtures. The resulting spectra provided information about the molecular nature of the extract and the molecular environment on the nanoparticle surface. Figure 4 shows representative FTIR spectra, with bands indexed, of pure carrot extract, and Ag nanoparticles synthesised from the carrot extract with and without 2% PVP in the reaction mixture. The FTIR spectra for the pure carrot extract

represented by Figure 4a showed bands at 3275 and 2925 cm^{-1} which were assigned to O–H stretching vibration of alcohols and phenols and C–H stretching vibration respectively. Other significant bands in the spectra included 1637, 1407 and 498 cm^{-1}, respectively assigned to C=O stretching, C–H bending, and OH out-of-plane deformation. Two other bands in the spectra were 1039 cm^{-1} (C–O) and 923 cm^{-1} (=C–H) vibrational modes. The two prominent bands observed in biologically synthesised Ag nanoparticles (without PVP) shown in Figure 4b were observed at 1320 and 1520 cm^{-1}. The 1320 cm^{-1} band was assigned to C–N stretching, and 1520 cm^{-1} was assigned to N–H bending, with the source of N being the $AgNO_3$. Also observed was a shift in the position of the bands between the pure carrot extracts and those from which Ag nanoparticles were synthesised. The shift was believed to be the result of the reduction of Ag^+ ions and subsequent formation of Ag nanoparticle. From the FTIR spectra and its detection in the XRD data, ascorbic acid seems to be the main agent involved in the reduction of the $AgNO_3$. Also, ascorbate ions, along with amines and alcohols present in the carrot extract appear to be responsible for capping and stabilising the synthesised Ag nanoparticles. The results are consistent with reports involving Ag nanoparticles synthesis from carrot extracts [27].

The effect of PVP during the reduction of $AgNO_3$ and the stabilisation of the synthesised Ag nanoparticles was also investigated using FTIR spectra of reactions which incorporated 0.5%, 1%, 1.5% and 2% PVP. Analyses of the respective spectra revealed they had similar spectral bands. The pronounced effect of the 2% PVP is demonstrated in the spectra presented in Figure 4c. They show bands at 3315 cm^{-1} and 2927 cm^{-1} which were assigned to O–H stretching and C–H stretching vibrations respectively. A strong band in the spectra was identified at 1635 cm^{-1} and was assigned to C=O stretching. This band, however, was more intense when compared to spectra of pure carrot extract and the Ag nanoparticles synthesised without PVP (Figure 4 a,b). The results indicate the existence of significant carbonyl oxygen which can bond with hydrogen. Bands in the spectra included 1424 cm^{-1}, 1290 cm^{-1} and 1043 cm^{-1}. The band 1424 cm^{-1} was assigned to CH_2 bending vibrations, while 1290 cm^{-1} and 1043 cm^{-1} were assigned to C–N vibrations. Important features of PVP were the C=O, C–N and CH_2 functional groups which make it an effective stabiliser, which prevents the nanoparticles from aggregating in aqueous and many non-aqueous solutions. The spectra for the reactive mixture with PVP also revealed a shift in the position of the bands from their original position in the pure carrot extract (Figure 4a) and the Ag nanoparticles synthesised from the carrot extract without PVP (Figure 4b). Again, this shift was attributed to molecules present in the respective samples, which influenced the reduction of Ag^+ ions. The FTIR spectra also indicated that PVP molecules might have also contributed to the capping and stabilisation of the synthesised Ag nanoparticles.

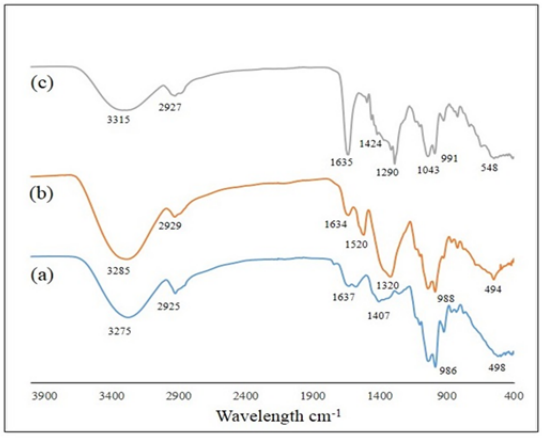

Figure 4. FTIR spectra of carrot extracts and Ag nanoparticles (a) spectra of carrot extract, (b) spectra of Ag nanoparticles synthesised from carrot extract, and (c) spectra of Ag nanoparticles synthesised from carrot extract containing 2% PVP.

3.5. Particle size and morphology of Ag nanoparticles

The sizes and morphology of the bio-reduced Ag nanoparticles were determined using transmission electron microscopy. Figure 5 is a representative transmission electron micrograph of Ag nanoparticles prepared from only carrot extract; it shows predominantly spherical and pseudo-spherical Ag nanoparticles, 2 to 25 nm in diameter. The small size range observed in the image indicated the nanoparticles were capped and stabilised. They were also somewhat dispersed with some small clusters present; the red circles in Figure 5 have highlighted these.

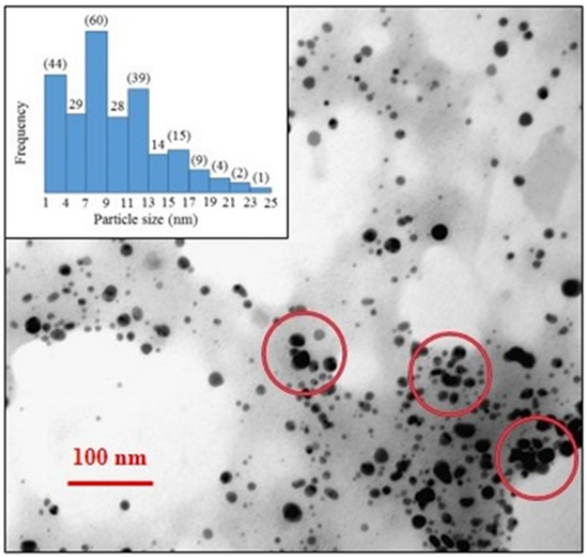

Figure 5. Distribution of Ag nanoparticles bio-synthesised from carrot extract with a frequency distribution of the particle sizes as determined from a representative sample using TEM.

The presence of PVP in the reaction mixtures had a significant influence on the morphology of the resulting Ag nanoparticles. This effect is seen in Figure 6a where the addition of 2% PVP produced nanoparticles of different shapes and a wider range of sizes. The pseudo-spherical particles were larger than those produced without PVP and ranged from 10 to 50 nm in diameter. The other nanoparticles observed were either triangular, cubic, polygons or rod-shaped and were between 10 to 35 nm wide (Figure 6a). A frequency distribution showed relatively more spherical, and polygonal nanoparticles were produced (Figure 6b,c). These results suggest the most probable mechanism for synthesis of these Ag nanoparticles involved the preferential coating of PVP on the {100} facets, which in turn promoted growth in particular orientations to produce specific nanoparticle shapes [43]. These observations confirm PVP as a shape-controlling agent with the ability to promote the growth of specific crystal facets while hindering the growth of other facets [42]. Also, there is an indication that PVP strongly binds to the {100} facets of Ag to promote growth along <111> directions to obtain a variety of nanometre-scale shapes as shown in Figure 6a. This role is consistent with studies which also show the carbonyl groups present in PVP tend to promote growth on the {100} facets, which helps to drive the growth in particular orientations to give specific morphologies [43,44]. These reports and the results in this study contradict that PVP coating does not preferentially adsorb on the {100} facets, but instead forms a homogeneous coating [45].

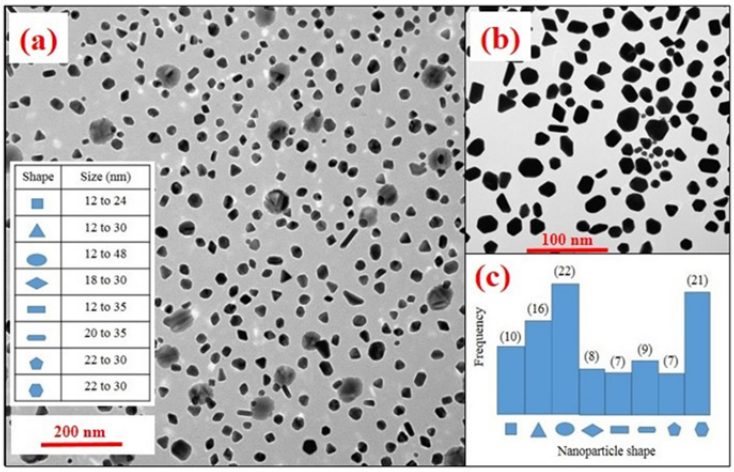

Figure 6. Distribution of Ag nanoparticles bio-synthesised from a carrot extract containing $AgNO_3$ and 2% PVP: (a) distribution of nanoparticles of different shapes and sizes; (b) enlarged image of (a) showing the dispersed nature of the particles and (c) frequency distribution of nanoparticle of discrete shapes from a representative sample of nanoparticles.

Another prominent feature of the Ag nanoparticles produced in the presence of PVP was that they were discrete and well dispersed. This characteristic is different from the nature of the nanoparticles synthesised from carrot extracts in studies where PVP was not used [25–27]. The results show PVP is a strong stabilizer, and have properties that prevent clustering or aggregation of the nanoparticles. This stabilising property is likely due to the polyvinyl backbone that incorporates a

repeating highly polar amide group that produces polar-attracting properties (hydrophilic nature) and a repeating non-polar methylene group that has hydrophobic properties. These non-polar methylene groups generate repulsive forces that extend outwards into the extract and interact with other nanoparticles to generate steric hindrance; this makes the generation of discrete and highly dispersed nanoparticles a feature of reaction mixtures that contain PVP.

3.6. Antibacterial activity of the synthesized Ag nanoparticles

The antibacterial activity of the synthesised Ag nanoparticles was tested against two bacteria; the gram-negative *E. coli* and the gram-positive *S. epidermidis* using the Kirby and Bauer disk diffusion method. Initially, both pathogens were evaluated against test disks treated with the carrot extract. The results indicated that the extract had no antibacterial properties because there was no zone of inhibition on the agar plates. However, when the bacteria were challenged with Ag nanoparticles produced from the various reaction mixtures, there was clear evidence of antibacterial activity against both microbes (Figure 7).

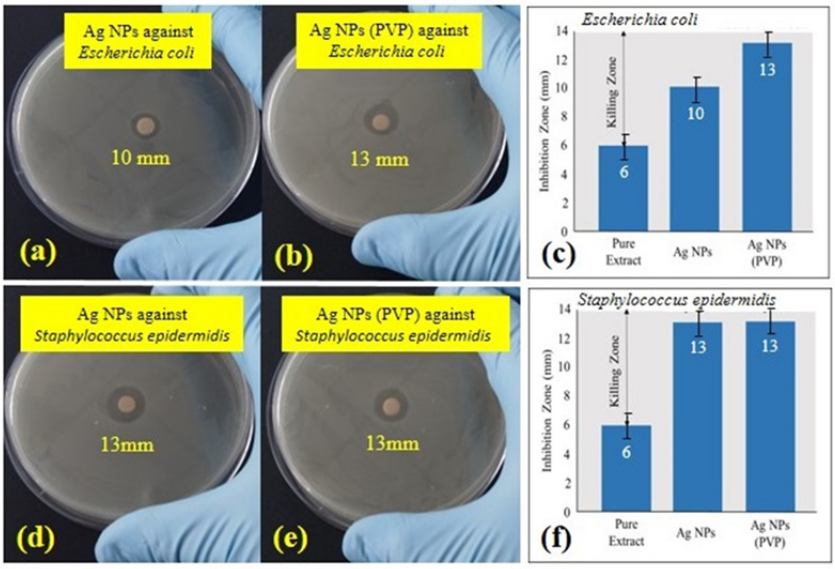

Figure 7. Antibacterial activity of Ag nanoparticles against *E. coli* and *S. epidermidis*: (a, b) Inhibition zones on *E. coli* plates induced by Ag nanoparticles synthesised with 1% PVP and without PVP, (d, e) Inhibition zones on S. epidermidis plates induced by Ag nanoparticles synthesised with and without PVP (c) Average diameters of inhibition zones against *E. coli* by pure carrot extract, and Ag nanoparticles (f) Average diameters of inhibition zones against *S. epidermidis* by pure carrot extract, and Ag nanoparticles.

The highest antibacterial activity for Ag nanoparticles generated from a reaction mixture containing carrot extract and $AgNO_3$ (volume ratio 1:1) was recorded for *S. epidermidis* with an inhibition zone of 13 mm. For *E. coli*, the highest activity with the same extract resulted in an inhibition zone of 10 mm. The antibacterial challenge also indicated the presence of PVP in the

reaction mixture improved the antibacterial activity against *E. coli*, increasing the zone of inhibition from 10 to 13 mm but had no apparent effect on *S. epidermidis* (Figure 7). Differences in the inhibition zones are most likely the result of the differences in the cell wall composition and structure of the gram-positive and gram-negative bacteria. The cell wall structure of gram-positive bacteria is rigid and is made up of a thick peptidoglycan layer composed of linear polysaccharide chains. These chains are cross-linked by short peptides, which makes it exceedingly difficult for Ag nanoparticles to penetrate the cell wall. The cell wall of gram-negative bacteria is, however, composed of a thin peptidoglycan layer, which offers less resistance to penetration of the Ag nanoparticles [46,47].

Three mechanisms are currently believed to contribute to the antibacterial activity of Ag nanoparticles. These are: (1) when Ag nanoparticles come into contact with the negatively charged bacterial cell wall, they change the physicochemical properties of the wall, which disturbs cell functions such as osmoregulation, permeability and respiration [48–52]; (2) Ag nanoparticles enter the cell and interact and disrupt cell components such as DNA and proteins [53,54]; and (3) the embedded Ag nanoparticles release Ag^+ ions that promote greater antibacterial activity [51,55,56]. However, the precise mechanisms involved and the influence of surface coatings of Ag nanoparticles needs further investigation. The involvement of Ag nanoparticles as a bacteriostatic agent was demonstrated for both *E. coli* and *S. epidermidis* as the zones of inhibition were increased by 67% and 117% respectively over that produced by the pure carrot extracts. These results indicate that Ag nanoparticles can interfere with the growth of bacteria. Whether the Ag nanoparticles synthesised with PVP promotes the antibacterial activity was not clear as it seems to have affected only the *E. coli*. The interaction and involvement of capping agents such as PVP in affecting the growth of bacteria need further investigation [53,57]. Information of these aspects is of particular importance as Ag nanoparticles are currently being favoured over conventional biomedical materials such as broad spectrum conventional antibiotics and these Ag nanoparticles/nanostructures can be synthesised by various pathways [58–60].

4. Conclusion

The study sought to investigate how two of the challenges facing the world could be solved in a cost-effective manner by using carrots, which would otherwise go waste, in producing nanoparticles, particularly silver nanoparticles which can be used as an alternative source to produce antimicrobial agents. The results demonstrated that with improvement in current green synthesis methods, it was possible to synthesise stable and discrete Ag nanoparticles of various shapes and sizes with bacteriostatic properties against two opportunistic human bacterial pathogens. The synthesis process is simple and can potentially be scaled up relatively easily. More investigation into the role of potential reducing agents, including ascorbic acid and ascorbate ions, and amines and alcohols that could act as capping agents may improve the synthesis process. Also, the antimicrobial properties of the nanoparticles demonstrated against *E. coli* and *S. epidermidis* is a good foundation for future investigation industrial applications.

One of the current ways of reducing carrot food waste in Australia is by ploughing excess or rejected produce into the soil as organic manure. It is important to note that such a practice is essential to maintain long term fertility of farming soils. The drive to reclaim as much value from carrots by

using it as a source for the production for useful silver nanoparticles will not necessarily interfere with its use by farmers as green manure. This is because the residues of the green synthesis process described in this study may still be readily available for use as manure without further processing, making this valorisation strategy for carrot a favourable proposal both in Australia and around the world.

Acknowledgements

Mrs Purabi Ghosh thanks Murdoch University for providing her with a PhD Scholarship. The authors also thank the Department of Primary Industry and Regional Development, DPIRD, Western Australia for their co-operation and access to their transmission electron microscopy facility.

Conflict of interests

The authors declare that there is no conflict of interest.

References

1. De M, Ghosh PS, Rotello VM (2008) Applications of nanoparticles in biology. *Adv Mater* 20: 4225–4241.
2. Salata OV (2004) Applications of nanoparticles in biology and medicine. *J Nanobiotechnol* 2: 3.
3. Stark WJ, Stoessel PR, Wohlleben W, et al. (2015) Industrial applications of nanoparticles. *Chem Soc Rev* 44: 5793–5805.
4. Zhao X, Meng Z, Wang Y, et al. (2017) Pollen magnetofection for genetic modification with magnetic nanoparticles as gene carriers. *Nat Plants* 3: 956–964.
5. Torney F, Trewyn BG, Lin VSY, et al. (2007) Mesoporous silica nanoparticles deliver DNA and chemicals into plants. *Nat Nanotechnol* 2: 295–300.
6. Shanmuganathan R, Karuppusamy I, Saravanan M, et al. (2019) Synthesis of Silver nanoparticles and their biomedical applications—A comprehensive review. *Cur Pharm Design* 25: 2650–2660.
7. Wong KKY, Liu XL (2010) Silver nanoparticles: the real "silver bullet" in clinical medicine? *MedChemComm* 1: 125–131.
8. Pugazhendhi A, Prabakar D, Jacob JM, et al. (2018) Synthesis and characterization of silver nanoparticles using Gelidium amansii and its antimicrobial property against various pathogenic bacteria. *Microb Pathogensis* 114: 41–45.
9. Ramkumara VS, Pugazhendhib A, Gopalakrishnanb K, et al. (2017) Bio-fabrication and characterization of silver nanoparticles using aqueous extract of seaweed Enteromorpha compressa and its biomedical properties. *Biotechnol Rep* 14: 1–7.
10. Levy SB, Marshall B (2002) Antibacterial resistance worldwide: causes, challenges and responses. *Nat Med* 12: S122–S129.
11. Chui CS, Cowling BJ, Lim WW, et al. (2020) Patterns of inpatient antibiotic use among public hospitals in Hong Kong from 2000 to 2015. *Drug Safety* 43: 595–606.

12. Tarannum N, Gautam YK (2019) Facile green synthesis and applications of silver nanoparticles: a state-of-the-art review. *RSC Adv* 9: 34926–34948.
13. Siddiqi KS, Husen A, Rao RAK (2018) A review on biosynthesis of silver nanoparticles and their biocidal properties. *J Nanobiotechnol* 16: 14.
14. Pethakamsetty L, Kothapenta K, Nammi HR, et al. (2017) Green synthesis, characterization and antimicrobial activity of silver nanoparticles using methanolic root extracts of Diospyros sylvatica. *J Environ Sci* 55: 157–163.
15. Jyoti K, Baunthiyal M, Singh A (2016) Characterization of silver nanoparticles synthesized using Urtica dioica Linn leaves and their synergistic effects with antibiotics. *J Radiat Res Appl Sc* 9: 217–227.
16. Ai J, Biazar E, Jafarpour M (2011) Nanotoxicology and nanoparticle safety in biomedical designs. *Int J Nanomed* 6: 1117–1127.
17. Gautama A, van Veggel FCJM (2013) Synthesis of nanoparticles, their biocompatibility, and toxicity behaviour for biomedical applications. *J Mater Chem B* 1: 5186–5200.
18. Meetoo DD (2011) Nanotechnology and the food sector: from the farm to the table. *Emir J Food Agr* 23: 387–403.
19. Nowack B (2009) The behaviour and effects of nanoparticles in the environment. *Environ Pollut* 157: 1063–1185.
20. Ghosh PR, Fawcett D, Sharma SB, et al. (2017) Production of high-value nanoparticles via biogenic processes using aquaculture & horticultural food wastes. *Materials* 10: 859–877.
21. Akhtar MS, Panwar J, Yun YS (2013) Biogenic synthesis of metallic nanoparticles by plant extracts. *ACS Sustain Chem Eng* 1: 591−602.
22. Australian Department of Agriculture (2014) Australian food statistics 2012–13. Available from: https://www.agriculture.gov.au/sites/default/files/sitecollectiondocuments/ag-food/publications/food-stats/australian-food-statistics-2012-13.pdf.
23. Hanson R (2014) Carrots turned into fertiliser because they are too big to sell. Available from: https://www.themercury.com.au/lifestyle/carrots-turned-into-fertiliser-because-they-are-too-big-to-sell/news-story/2b1fd17e99031e07f6ea7df78285162d.
24. Jacob JM, John MS, Jacob A, et al. (2019) Bactericidal coating of paper towels via sustainable biosynthesis of silver nanoparticles using Ocimum sanctum leaf extract. *Mater Res Express* 6: 045401.
25. Shanmuganathan R, MubarakAli D, Prabakar D, et al. (2018) An enhancement of antimicrobial efficacy of biogenic and ceftriaxone-conjugated silver nanoparticles: green approach. *Environ Sci Pollut R* 25: 10362–16370.
26. Abubakar AS, Salisu IB, Chahal S, et al. (2014) Biosynthesis and characterization of silver nanoparticles using black carrot root extract. *IJCRR* 6: 5–8.
27. Umadevi M, Shalini S, Bindhu MR (2012) Synthesis of silver nanoparticle using *D. Carota* extract. *Adv Nat Sci-Nanosci* 3: 025008.
28. Bauer AW, Kirby WM, Sherris JC (1996) Antibiotic susceptibility testing by a standardized single disk method. *Am J Clin Pathol* 45: 493–496.

29. Sotto A, De Boever CM, Fabbo-Peray P, et al. (2001) Risk factors for antibiotic-resistant Escherichia coli isolated from hospitalised patients with urinary tract infections: a prospective study. *J Clin Microbiol* 39: 438–444.
30. Otto M (2009) Staphylococcus epidermidis–the accidental pathogen. *Nat Rev Microbiol* 7: 555–567.
31. Kanipandian N, Kannan S, Ramesh R, et al. (2014) Characterization, antioxidant and cytotoxicity evaluation of green synthesized silver nanoparticles using Cleistanthus collinus extract as surface modifier. *Mater Res Bull* 49: 494–502.
32. Ahmad N, Sharma S (2012) Green synthesis of silver nanoparticles using extracts of Ananas comosus. *GSC* 2: 141–147.
33. Muthukrishnan S, Bhakya S, Senthil Kumar T, et al. (2015) Biosynthesis, characterization and antibacterial effect of plant-mediated silver nanoparticles using Ceropegia thwaitesii—An endemic species. *Ind Crop Prod* 63: 119–124.
34. Samuel MS, Jose S, Selvarajan E, et al. (2020) Biosynthesized silver nanoparticles using Bacillus amyloliquefaciens; Application for cytotoxicity effect on A549 cell line and photocatalytic degradation of p-nitrophenol. *J Photochem Photobio B* 202:111642.
35. Vigneshwaran N, Ashtaputre N, Varadarajan P, et al. (2007) Biological synthesis of silver nanoparticles using the fungus Aspergillus flavus. *Mater Lett* 61: 1413–1418.
36. Zidorn C, Johrer K, Ganzera M (2005) Polyacetylenes from the Apiaceae vegetables carrot, celery, fennel, parsley, and parsnip and their cytotoxic activities. *J Agr Food Chem* 53: 2518–2523.
37. Alasalvar C, Grigor JM, Zhang D (2001) Comparison of volatiles, phenolics, sugars, antioxidant vitamins, and sensory quality of different coloured carrot varieties. *J Agr Food Chem* 49: 1410–1416.
38. Zhang D, Hamauzu Y (2004) Phenolic compounds and their antioxidant properties in different tissues of carrots (*Daucus carota* L.). *J Food Agric Environ* 2: 95–100.
39. Li LL, Tang RC (2017) A chlorogenic acid mediated synthesis of silver nanoparticles and their application for the antibacterial functionalization of silk fiber. *Proceedings of the 2017 2nd International Conference on Materials Science, Machinery and Energy Engineering* 123: 781–784.
40. Wang M, Zhang W, Zheng X (2017) Antibacterial and catalytic activities of biosynthesized silver nanoparticles prepared by using an aqueous extract of green coffee bean as a reducing agent. *RSC Adv* 7: 12144–12149.
41. Isaac RS, Sakthivel G (2013) Green synthesis of gold and silver nanoparticles using *Averrhoa bilimbi* fruit extract. *J Nanotechnol* 2013: 906592.
42. Martınez-Castanon GA, Nino-Martınez N, Martınez-Gutierrez F (2008) Synthesis and antibacterial activity of silver nanoparticles with different sizes. *J Nanopart Res* 10: 1343–1348.
43. Thanh N, Maclean N, Mahiddine S (2014) Mechanisms of nucleation and growth of nanoparticles in solution. *Chem Rev* 114: 7610–7630.
44. Papp S, Patakfalvi R, Dekanya I (2007) Formation and stabilization of noble metal nanoparticles. *Croat Chem Acta* 80: 493–502.

45. Xia Y, Xiong Y, Lim B, et al. (2009) Shape-controlled synthesis of metal nanocrystals: Simple chemistry meets complex physics? *Angew Chem Int Edit* 48: 60–103.
46. Rycenga M, Cobley CM, Zeng J (2011) Controlling the synthesis and assembly of silver nanostructures for plasmonic applications. *Chem Rev* 111: 3669–3712.
47. Choi YH, Chae YS, Lee JH (2015) Mechanism of metal nanowire formation via the polyol process. *Electron Mater Lett* 11: 735–740.
48. Shrivastava S, Bera T, Roy A, et al. (2007) Characterization of enhanced antibacterial effects of novel silver nanoparticles. *Nanotechnology* 18: 103–112.
49. Mubarak Ali D, Tahjuddin N, Jeganathan K, et al. (2011) Plant extract mediated synthesis of silver and gold nanoparticles and its antibacterial activity against clinically isolated pathogens. *Colloid Surface B* 85: 360–365.
50. Dibrov P, Dzioba J, Gosink KK (2002) Chemiosmotic mechanism of antimicrobial activity of Ag^+ in vibrio cholera. *Antimicrob Agents Ch* 46: 2668–2670.
51. Sondi I, Salopek-Sondi B (2004) Silver nanoparticles as antimicrobial agent: a case study on E. coli as a model for gram-negative bacteria. J Coll Interface Sci 275: 177–182.
52. Nel AE, Madler L, Velegol D, et al. (2009) Understanding biophysicochemical interactions at the nano-bio interface. *Nat Mater* 8: 543–557.
53. Su HL, Chou CC, Hung DJ, et al. (2009) The disruption of bacterial membrane integrity through ROS generation induced by nanohybrids of silver and clay. *Biomaterials* 30: 5979–5987.
54. Marambio-Jones C, Hoek EMV (2010) A review of the antibacterial effects of silver nanomaterials and potential implications for human health and the environment. *J Nanopart Res* 12: 1531–1551.
55. AshaRani PV, Mun GLK, Hande MP, et al. (2009) Cytotoxicity and genotoxicity of silver nanoparticles in human cells. *ACS Nano* 3: 279–290.
56. Subhasree B, Baskar R, Keerthana RL, et al. (2009) Evaluation of antioxidant potential in selected green leafy vegetables. *Food Chem* 115: 1213–1220.
57. Liu JY, Sonshine DA, Shervani S, et al. (2010) Controlled release of biologically active silver from nanosilver surfaces. *ACS Nano* 4: 6903–6913.
58. Jones RS, Draheim RR, Roldo M (2018) Silver nanowires: synthesis, antibacterial activity and biomedical applications. *Appl Sci* 8: 673–688.
59. Hernandez-Sierra JF, Ruiz F, Pena DC, et al. (2008) Antimicrobial sensitivity of Streptococcus mutants to nanoparticles of silver, zinc oxide and gold. *Nanomedicine* 4: 237–240.
60. Saravanan M, Barik SK, MubarakAli D, et al. (2018) Synthesis of silver nanoparticles from Bacillus brevis (NCIM 2533) and their antibacterial activity against pathogenic bacteria. *Microb Pathogenesis* 116: 221–226.

AIMS Press